

Institute for Software Integrated Systems
Vanderbilt University
Nashville, Tennessee, 37235

Multi-Rate Networked Control of Conic Systems

Nicholas Kottenstette, Heath LeBlanc, Emeka Eyisi, Xenofon Koutsoukos

TECHNICAL REPORT

ISIS-09-108

Abstract—Implementation uncertainties such as time-varying delay and data loss and having to typically implement a discrete-time-controller can cause significant problems in the design of networked control systems. This paper describes a novel multi-rate digital-control system which preserves stability and provides robustness to such implementation uncertainties. We present necessary conditions for stability of conic systems interconnected over digital-control-networks which can tolerate networked delays and data-loss. We also compare the performance using simulation results of the proposed architecture to that of a classic-digital-control-implementation applied to controlling position of a single-degree of freedom robotic manipulator.

I. INTRODUCTION

The heterogeneous composition of computing, sensing, actuation, and communication components has enabled a vision for real-world Cyber Physical Systems such as automotive vehicles, building automation systems, and groups of unmanned air vehicles. Such systems are monitored and controlled by Networked Control Systems (NCS) that integrate computational and physical devices using communication networks. NCS research has been recently a very active area investigating problems at the intersection of control systems, networking, and computer science [1].

The objective of this paper is to address fundamental problems in NCS caused by implementation uncertainties such as time-varying delay, and data loss. To deal with these implementation uncertainties, we propose a design approach on top of passivity [2]. The inherent safety that passive systems provide is fundamental in building systems that are insensitive to implementation uncertainties.

Our team has investigated the use of passivity for the design of NCS investigating stability in the presences of time-varying delays [3], [4]. This paper presents an important new step in the design of networked control systems consisting of multiple plants by considering conic systems that relax the passivity assumptions. Passive systems are a special case of conic systems, thus the paper expands the applicability of our framework. Further, conic systems can be used to represent many important application such as quadrotor aircraft [5].

Our approach employs wave variables to transmit information over the network for the feedback control while remaining passive when subject to arbitrary fixed time delays and data dropouts [6], [7]. The primary advantage of using wave variables is that they tolerate most time-varying delays, such as those occurred when using the TCP/IP transmission protocol. In addition, our architecture adopts a multi-rate digital control scheme to account for different time scales at different part of the network as well as bandwidth constraints.

This paper provides necessary conditions for stability of conic systems to be interconnected over wireless networks which can tolerate networked delays, and data-loss. The continuous-time bounded results can be achieved for all linear and nonlinear conic systems. The paper also demonstrates how the proposed architecture can implemented using a new

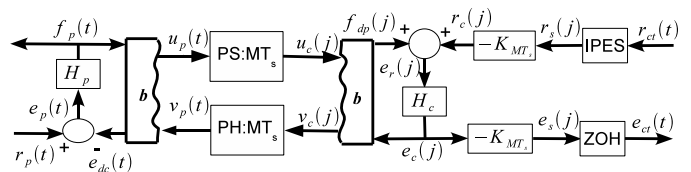


Fig. 1. High Performance, multi-rate digital control network for continuous-time systems.

linear passive-sampler. Finally, our architecture can be used to isolate wide-band and correlated noise without affecting stability through the use of a discrete-time anti-aliasing-filter $H_{LP}(z)$ which was synthesized by applying the conic-preserving-IPESH-Transform to a high-order Butterworth filter $H_{LP}(s)$.

Section II describes our new high-performance digital control system and provides all the necessary analysis and stability results. Section III describes a position-control problem involving a single-degree of freedom robotic manipulator problem in order to compare our proposed-architecture to that of a classic-digital-control-implementation. Section IV presents the simulation results. Section V provides the conclusions of our paper.

II. HIGH PERFORMANCE DIGITAL CONTROL NETWORKS

Fig. 1 depicts a multi-rate digital control network which interfaces a conic-digital-controller $H_c : e_r \rightarrow e_c$ to a continuous-time conic plant $H_p : e_p \rightarrow f_p$ [5], [8], [9]. The digital control network is a hybrid-network consisting of both continuous-time wave variables ($u_p(t), v_p(t)$) and discrete-time wave variables ($u_c(j), v_c(j)$) in which $j = \lfloor \frac{t}{MT_s} \rfloor$ [6], [7], [10]. The relationships between the continuous-time and discrete-time wave variables is determined by the multi-rate-passive-sampler (denoted PS : MT_s) and multi-rate-passive-hold (denoted PH : MT_s). These two elements are combination of the passive-sampler and passive-hold blocks (which have been instrumental in showing how to interconnect digital-controllers to continuous-time systems in order to achieve L_m^2 -stability [3], [10] see [11], [12] for interconnecting continuous time-plants to continuous-time-controllers over digital networks) and a discrete-time passive-up-sampler and passive-down-sampler [4]. At the interface to the digital controller is an inner-product-equivalent sample and zero-order hold block $e_{ct}(t) = e_s(j)$, $t \in [jMT_s, (j+1)MT_s)$ [10] which are used for analysis in order to relate continuous-time-control-inputs $r_{ct}(t)$ and continuous-time-control-outputs $e_{ct}(t)$ to the continuous-time-plant inputs $r_p(t)$ and outputs $f_p(t)$.

The architecture has the following advantages over traditional digital control systems:

- 1) continuous-time bounded-stability results can be achieved for all linear and non-linear conic systems H_c which are inside the sector $[a_c, b_c]$ in which $-\infty < a_c < b$, $0 \leq b \leq \infty$,
- 2) wide-band, and correlated noise introduced into the signal $f_p(t)$ can be effectively isolated using the multi-

rate-passive-sampler before implementing the high-gain digital-controller H_c without adversely affecting stability,

3) we show that the *IPESH*-Transform preserves the conic-properties of a reference analog filter in the discrete-time domain in order to synthesize discrete-time-anti-aliasing filters based on Butterworth filter models.

By choosing, to use wave-variables, a negative output feed-back loop is introduced for both the plant and controller in which we provide the necessary analysis to determine its effects in Section II-A. This analysis in which we consider boundedness results for *digital control* is inspired by the insightful *continuous-time control* results presented in [13] in which the plant-disturbance *was not considered* ($r_p(t) = 0$). Section II-B introduces the multi-rate-passive-sampler and multi-rate-passive-hold which includes a *new linear* passive-sampler which will encourage further analysis and simplify implementation, it also includes are main stability results. Section II-C provides the necessary results to construct conic-digital-filters (which are inside the sector $[a_f, b_f]$ from conic-continuous-time-filters which are also inside the sector $[a_f, b_f]$).

A. Control of a Conic System Cascaded With a Passive System

Many continuous-time dynamical systems denoted by the symbol $H_s : u_s \rightarrow y_p$ (in which $u_s \in \mathbb{R}^m$ is an input-function in the extended L_2^m -space and $H_s u_s = y_p \in \mathbb{R}^m$ denotes an image of u_s under H_s each with instantaneous values at time $t \in \mathbb{R}$ denoted as $u_s(t)$ and $y_p(t)$ respectively) can typically be described by a cascade of a conic-system $H_c : u_s \rightarrow y_c$ which precedes a passive system $H_p : y_c \rightarrow y_p$. A passive system is a special type of conic-system which can be contained inside a positive sector $[0, \infty]$. When each sub-system H_c and H_p can be described by a set of ordinary differential equations of the following general form with input $u \in \mathbb{R}^m$, output $y \in \mathbb{R}^m$, and state $x \in \mathbb{R}^n$

$$\begin{aligned} \dot{x}(t) &= F(x(t), u(t)), \quad x(t_0) = x_0, \quad t \geq t_0 \\ y(t) &= H(x(t), u(t)) \end{aligned} \quad (1)$$

and in addition if $F(0, 0) = 0$, $H(0, 0) = 0$ and a positive-definite storage function $V(x(t)) > 0$, $V(0) = 0$ exists which is continuously differentiable such that $\dot{V}(x(t)) \leq r(u(t), y(t))$ $t \geq 0$ holds, then each subsystem is a dissipative-system [14, Corollary 5.1 (5.31)] with respect to the (conic) supply rate $r(u(t), y(t))$ $-\infty < a < \infty$ $|a| < b \leq \infty$ in which the conic-supply-rate is of the following form:

$$r(u(t), y(t)) = y^\top(t)u(t) - \frac{1}{a+b}y^\top(t)y(t) - \frac{ab}{a+b}u^\top(t)u(t). \quad (2)$$

We chose to restrict ourselves to the less general conic-supply-rates as they allow us to leverage the earlier work of [8] and [9] when studying bounded-stability for conic-systems $H : u \rightarrow y$ which are inside the sector $[a, b]$ in which the previous constraints on a and b hold such that:

$$\|(y)_T\|_2^2 - (a+b)\langle y, u \rangle_T + (ab)\|(u)_T\|_2^2 \leq 0 \text{ holds } \forall T \geq 0. \quad (3)$$

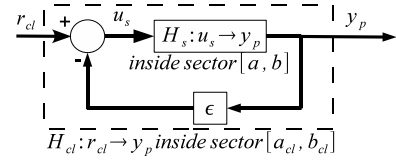


Fig. 2. Nominal closed-loop system H_{cl} resulting from ϵ and H_s .

Conic-systems are not in general dissipative, however, if a dissipative-system has a conic-supply-rate then it is a conic-system [5, Remark 3]. There are cases when H_c is a dissipative-conic-system in which $|a| < b < \infty$ and H_p is a passive-system and the resulting cascaded system H_s is a dissipative-conic-system inside the sector $[a, b]$ in which b is typically finite when H_p is strictly-output passive. For, example, a linear-time-invariant system which describes the position $Y_p(s)$ of a unit-mass which is subject to a force $U_s(s)$ consists of a double integrator $H_s(s)$.

$$H_s(s) = H_c(s)H_p(s) = \frac{Y_c(s)Y_p(s)}{U_s(s)Y_c(s)} = \frac{Y_p(s)}{U_s(s)} = \frac{1}{s} \frac{1}{s} = \frac{1}{s^2}. \quad (4)$$

A Nyquist plot will quickly show that although both H_c and H_p are passive integrators the resulting system $H_s(s)$ is not a conic-system in which there does not exist an $|a| < \infty$ to contain H_s inside the sector $[a, \infty]$. In order make $|a|$ finite, H_c is made strictly output-passive by simply closing the loop on $k_c \frac{1}{s}$ such that $H_c(s) = \frac{k_c}{s+k_c}$. The resulting system $H_s(s) = \frac{k_c}{s(s+k_c)}$ can be shown to be inside the sector $[-\frac{1}{k_c}, \infty]$ $k_c > 0$.

We are particularly interested in determining the resulting gain $g(H_{cl})$ ($\|(y_c)_T\|_2 \leq g(H_{cl})\|(r_c)_T\|_2$) when closing the loop of a conic-system H_s which is inside the sector $[a, b]$ as depicted in Fig. 2.

Theorem 1: The conic-system $H_s : u_s \rightarrow y_p$ depicted in Fig. 2 is inside the sector $[a, b]$, $\epsilon > 0$. The input u_s is related to the reference r_s and output y_p by the following feedback equation

$$u_s(t) = r_s(t) - y_p(t), \quad \forall t \geq 0.$$

The resulting closed-loop system is denoted $H_{cl} : r_s \rightarrow y_p$. For the case when:

- I. $0 \leq a < b \leq \infty$, H_{cl} is inside the sector $[\frac{a}{1+\epsilon a}, \frac{b}{1+\epsilon b}]$ in which $g(H_{cl}) = \frac{b}{1+\epsilon b}$.
- II. $a < 0$, $-a < b \leq \infty$, $-1 < 2\epsilon a < 0$, and $b > -\frac{a}{1+2\epsilon a}$ then H_{cl} is inside the sector $[\frac{a}{1+\epsilon a}, \frac{b}{1+\epsilon b}]$ in which $g(H_{cl}) = \frac{b}{1+\epsilon b}$.

Proof:

- I. We recall the relationship for our conic-system H_s that

$$\langle y_p, u_s \rangle_T \geq \frac{1}{a+b}\|(y_p)_T\|_2^2 + \frac{ab}{a+b}\|(u_s)_T\|_2^2$$

substituting in the feed-back equation for u_s results in

$$\langle y_p, r_{cl} \rangle_T \geq \left(\epsilon + \frac{1}{a+b} \right) \|(y_p)_T\|_2^2 + \frac{ab}{a+b}\|(r_{cl} - \epsilon y_p)_T\|_2^2$$

solving for the norm of the feedback-error results in

$$\frac{a+b+2\epsilon ab}{a+b} \langle y_p, r_{cl} \rangle_T \geq \frac{1+\epsilon(a+b)+\epsilon^2 ab}{a+b} \|(y_p)_T\|_2^2 + \frac{ab}{a+b} \|(r_{cl})_T\|_2^2$$

cross multiplying results in the final expression

$$\langle y_p, r_{cl} \rangle_T \geq \frac{1}{a_{cl}+b_{cl}} \|(y_p)_T\|_2^2 + \frac{a_{cl}b_{cl}}{a_{cl}+b_{cl}} \|(r_{cl})_T\|_2^2$$

$$\text{in which } a_{cl} = \frac{a}{1+\epsilon a}, \quad b_{cl} = \frac{b}{1+\epsilon b}.$$

II. We observe that as long as $a < 0$, $-a < b \leq \infty$, $-1 < 2\epsilon a < 0$, and $b > -\frac{a}{1+2\epsilon a}$ hold then all the inequalities used to determine the bounding sector for the previous case when $0 \leq a < b \leq \infty$ do indeed hold.

All that remains is to determine $g(H_{cl})$ in terms of a_{cl} and b_{cl} for both cases. From [5, Corollary 1] we know that H_{cl} is inside the sector $[a_{cl}, b_{cl}]$ if and only if it is interior conic with center $c = \frac{a_{cl}+b_{cl}}{2}$ and radius $r = \frac{b_{cl}-a_{cl}}{2}$ such that

$$\|(y_p - cr_{cl})_T\|_2 \leq r \|(r_{cl})_T\|_2, \quad \text{holds } \forall T \geq 0.$$

Which implies that

$$c \|(r_{cl})_T\|_2 + \|(y_p - cr_{cl})_T\|_2 \leq (c+r) \|(r_{cl})_T\|_2, \quad \forall T \geq 0.$$

We observe that under both cases the center $c > 0$, therefore, we can apply the triangle inequality to show that

$$\|(y_p + (c-c)r_{cl})_T\|_2 = \|(y_p)_T\|_2 \leq (c+r) \|(r_{cl})_T\|_2.$$

In which

$$g(H_{cl}) = c+r = \frac{a_{cl}+b_{cl}+b_{cl}-a_{cl}}{2} = b_{cl}. \quad \blacksquare$$

1) *Wave Variable Networks*: In order to analyze the closed-loop effects on H_p and H_c we recall our use of wave-variables. As discussed in [10] scattering [15] or their reformulation known as the wave-variable-networks allow *effort* and *flow* variables $(e_c(j), f_p(t))$, to be transmitted over a network while remaining *passive* when subject to arbitrary fixed time delays and data dropouts [6].

$$u_p(t) = \frac{1}{\sqrt{2b}} (bf_p(t) + e_{dc}(t)) \quad (5)$$

$$v_p(t) = \frac{1}{\sqrt{2b}} (bf_p(t) - e_{dc}(t)) \quad (6)$$

$$v_c(j) = \frac{1}{\sqrt{2b}} (bf_{dp}(j) - e_c(j)) \quad (7)$$

$$u_c(j) = \frac{1}{\sqrt{2b}} (bf_{dp}(j) + e_c(j)) \quad (8)$$

(5) can be thought of as the effective sensor output in a *wave variable* form for the plant H_p depicted in Fig. 1. Likewise, (7) can be thought of as the command output in a *wave variable* form from the controller H_c depicted in Fig. 1. (5) and (6) respectively satisfy the following equality:

$$\frac{1}{2} (u_p^T(t)u_p(t) - v_p^T(t)v_p(t)) = f_p^T(t)e_{dc}(t) \quad (9)$$

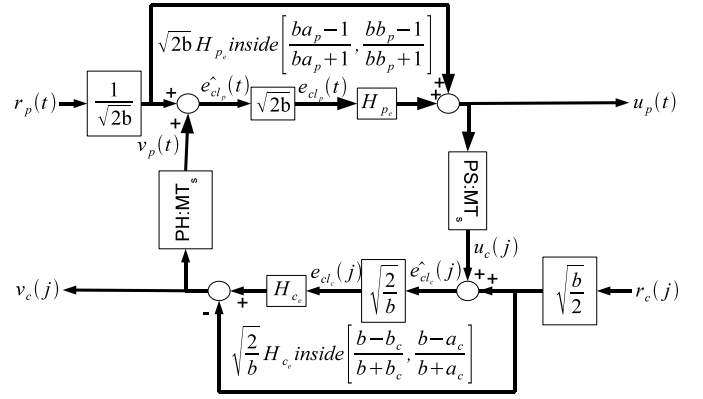


Fig. 3. Final Controller-Plant-wave-network realization.

Similarly, (7) and (8) respectively satisfy the following equality:

$$\frac{1}{2} (u_c^T(j)u_c(j) - v_c^T(j)v_c(j)) = f_{dp}^T(j)e_c(j). \quad (10)$$

Denote $I \in \mathbb{R}^{m_s \times m_s}$ as the identity matrix. When implementing the wave variable transformation the continuous time plant “outputs” $(u_p(t), e_{dc}(t))$ are related to the corresponding “inputs” $(v_p(t), f_p(t))$ as follows (Fig. 1):

$$\begin{bmatrix} u_p(t) \\ e_{dc}(t) \end{bmatrix} = \begin{bmatrix} -I & \sqrt{2b}I \\ -\sqrt{2b}I & bI \end{bmatrix} \begin{bmatrix} v_p(t) \\ f_p(t) \end{bmatrix} \quad (11)$$

Next, the discrete time controller “outputs” $(v_c(j), f_{dp}(j))$ are related to the corresponding “inputs” $(u_c(j), e_c(j))$ as follows (Fig. 1):

$$\begin{bmatrix} v_c(j) \\ f_{dp}(j) \end{bmatrix} = \begin{bmatrix} I & -\sqrt{\frac{2}{b}}I \\ \sqrt{\frac{2}{b}}I & -\frac{1}{b}I \end{bmatrix} \begin{bmatrix} u_c(j) \\ e_c(j) \end{bmatrix} \quad (12)$$

It has been shown that when a discrete-time-strictly-output-passive controller H_c is connected to a continuous-time-strictly-output-passive plant H_p over a wave-variable network which includes a passive-sampler and passive-hold and uses a *IPESH* for analysis, that the resulting network is L_m^2 -stable [3], [10]. In proving this we were able to, for a large part, ignore the underlying network structure which resulted from using the wave transform. In order to examine the case when H_p is not passive we need to explicitly consider the resulting network structure which results from the wave-variable transformation. In order to simplify discussion and create an explicit network structure as depicted in Fig. 3, which can leverage Theorem 1, we make the following assumptions:

Assumption 1: The scattering gain b must always satisfy the following bounds:

$$0 < b < \infty, \quad \text{if } a_p \geq 0 \\ 0 < b < \min\left\{-\frac{a_p+b_p}{2a_p}, -\frac{1}{2a_p}\right\}, \quad \text{if } a_p < 0.$$

In addition it is assumed that $a_c \geq 0$.

Which allows us to state the following theorem which is a direct result of Lemma 4 and Lemma 5:

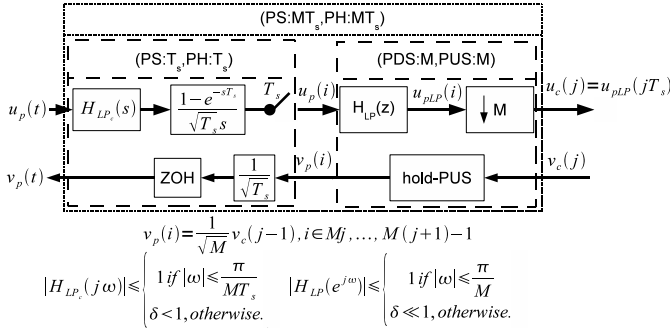


Fig. 4. Multi-rate passive-sampler, passive-hold.

Theorem 2: The plant-controller-network depicted in Fig. 1 can be transformed to the final form depicted in Fig. 3. In addition if Assumption 1 is satisfied, then

$$\sqrt{2b}H_{p_e} \text{ is inside the sector } \begin{bmatrix} ba_p - 1 & bb_p - 1 \\ ba_p + 1 & bb_p + 1 \end{bmatrix} \text{ and} \quad (13)$$

$$\sqrt{\frac{2}{b}}H_{c_e} \text{ is inside the sector } \begin{bmatrix} b - b_c & b - a_c \\ b + b_c & b + a_c \end{bmatrix}. \quad (14)$$

B. Multi-Rate-Passive-Sampler(Hold)

Fig. 4 depicts our proposed multi-rate passive-sampler (PS:MT_s), and passive-hold (PH:MT_s) subsystem. The multi-rate passive-sampler (PS:MT_s) consists of a cascade of a linear-passive-sampler (linear-PS:T_s) and a passive-downsampler (PDS:T_s). The multi-rate passive-hold (PH:MT_s) subsystem consists of a cascade of a passive-up-sampler (PUS:M) and passive-hold (PH:T_s). For simplicity of discussion the figure is for the single-input-single-output (SISO) case but we note all elements depicted can be diagonalized to handle *m*-dimensional waves. The standard anti-aliasing down-sampler ($H_{LP}(z), \downarrow M$) system depicted in Fig. 4 has been shown to be a PDS, in addition the hold-PUS depicted is a PUS [4, Definition 4]. A valid PDS:*M* and PUS:*M* satisfy the following inequalities:

$$\|(u_c(j))_N\|_2^2 \leq \|(u_p(i))_{MN}\|_2^2 \quad (15)$$

$$\|(v_p(i))_{MN}\|_2^2 \leq \|(v_c(j))_N\|_2^2 \quad (16)$$

which hold $\forall N \geq 0$. The scaled-ZOH block in which

$$v_p(t) = \frac{1}{T_s} v_p(i), \quad t \in [iT_s, (i+1)T_s)$$

has been shown to be a valid passive-hold system PH:T_s in which

$$\|(v_p(t))_{MNT_s}\|_2^2 \leq \|(v_p(i))_{MN}\|_2^2 \quad (17)$$

[3]. A valid passive-sampler will satisfy the following inequality

$$\|(u_p(i))_{MN}\|_2^2 \leq \|(u_p(t))_{MNT_s}\|_2^2, \quad (18)$$

unlike the non-linear averaging-passive-sampler [16, Definition 6] implementation which was shown to be a valid PS we choose to implement a linear version.

Definition 1: The linear-passive-sampler as depicted in Fig. 4 with input $u_p(t)$ and output denoted $u_p(i)$ is implemented as follows:

1. the input $u_p(t)$ is first filtered by an analog-low-pass-anti-aliasing filter denoted $H_{LP_c}(s)$ whose magnitude $|H_{LP_c}(j\omega)| \leq 1$ and unity-bandwidth should be roughly the digital-control-nyquist-frequency $\omega_n = \frac{\pi}{MT_s}$. The magnitude-roll-off should be one which achieves the desired-stop-band magnitude at $\omega = \frac{\pi}{T_s}$ (the nyquist-frequency of the second-stage digital anti-aliasing filter $H_{LP}(z)$).
2. the output of $H_{LP_c}(s)$ we denote as $u_{pLP_c}(t)$ in which

$$u_p(i) = \frac{1}{\sqrt{T_s}} \int_0^{iT_s} (u_{pLP_c}(t) - u_{pLP_c}(t - T_s)) dt \quad (19)$$

Lemma 1: The linear-passive-sampler (Definition 1) satisfies (18).

Proof: Since $u_p(t) = 0, t < 0$ by assumption, and the low-pass-filter is assumed to be causal therefore $u_p(0) = 0$ which implies that

$$0 = \|(u_p(i))_0\|_2^2 \leq \|(u_p(t))_0\|_2^2.$$

Next, we note that (19) can be equivalently written as

$$u_p(i) = \frac{1}{\sqrt{T_s}} \int_{(i-1)T_s}^{iT_s} u_{pLP_c}(t) dt$$

squaring both sides we have

$$u_p^2(i) = \frac{1}{T_s} \left(\int_{(i-1)T_s}^{iT_s} u_{pLP_c}(t) dt \right)^2$$

applying the Schwarz Inequality we have

$$u_p^2(i) \leq \frac{T_s}{T_s} \int_{(i-1)T_s}^{iT_s} u_{pLP_c}^2(t) dt$$

therefore

$$\begin{aligned} \|(u_p(i))_{MN}\|_2^2 &= \sum_{i=0}^{MN-1} u_p^2(i) \\ &\leq \sum_{i=0}^{MN-1} \int_{(i-1)T_s}^{iT_s} u_{pLP_c}^2(t) dt \\ &\leq \|(u_{pLP_c}(t))_{(MN-1)T_s}\|_2^2 \\ &\leq \|(u_{pLP_c}(t))_{MNT_s}\|_2^2 \end{aligned}$$

since the low-pass-filter has a gain less than or equal to one ($\|(u_{pLP_c}(t))_{MNT_s}\|_2^2 \leq \|(u_p(t))_{MNT_s}\|_2^2$) then (18) clearly results from these last two inequalities. ■

Finally, from (15) and (18) it is obvious that the following inequality holds for the multi-rate-passive-sampler PS:MT_s

$$\|(u_c(j))_N\|_2^2 \leq \|(u_p(t))_{MNT_s}\|_2^2 \quad (20)$$

and from (17) and (16) the following holds for the multi-rate-passive-hold PH:MT_s

$$\|(v_p(t))_{MNT_s}\|_2^2 \leq \|(v_c(j))_N\|_2^2 \quad (21)$$

With these two inequalities established, and Theorem 2 we can now prove the following Lemma.

Lemma 2: Denote the L_m^2 -gain of the plant-subsystem $H_{p_e} : \hat{e}_{cl_p} \rightarrow y_{p_e}$ as γ_{p_e} in which $\|(y_{p_e})_{MNT_s}\|_2 \leq \gamma_{p_e} \|(\hat{e}_{cl_p})_{MNT_s}\|_2$. In addition, denote the l_m^2 -gain of the controller-subsystem $H_{c_e} : \hat{e}_{cl_c} \rightarrow y_{c_e}$ as γ_{c_e} in which $\|(y_{c_e})_N\|_2 \leq \gamma_{c_e} \|(\hat{e}_{cl_c})_N\|_2$. In addition we shall use the following shorthand notation in which $E_p = \|(\hat{e}_{cl_p})_{MNT_s}\|_2$, $E_c = \|(\hat{e}_{cl_c})_N\|_2$, $R_p = \|(r_p)_{MNT_s}\|_2$, and $R_c = \|(r_c)_N\|_2$. If $\gamma_{p_e} \gamma_{c_e} < 1$ then

$$E_c \leq \frac{\gamma_{p_e} + 1}{1 - \gamma_{p_e} \gamma_{c_e}} \left(\sqrt{\frac{b}{2}} R_c + \frac{1}{\sqrt{2b}} R_p \right)$$

$$E_p \leq \frac{\gamma_{c_e} + 1}{1 - \gamma_{p_e} \gamma_{c_e}} \left(\sqrt{\frac{b}{2}} R_c + \frac{1}{\sqrt{2b}} R_p \right)$$

Proof: From the triangle inequality we have:

$$\|(\hat{e}_{cl_p})_{MNT_s}\|_2 \leq \frac{1}{\sqrt{2b}} \|(r_p)_{MNT_s}\|_2 + \|(v_p)_{MNT_s}\|_2 \quad (22)$$

$$\|(\hat{e}_{cl_c})_N\|_2 \leq \sqrt{\frac{b}{2}} \|(r_c)_N\|_2 + \|(u_c)_N\|_2 \quad (23)$$

$$\|(u_c)_N\|_2 \leq \gamma_{p_e} \|(\hat{e}_{cl_p})_{MNT_s}\|_2 + \frac{1}{\sqrt{2b}} \|(r_p)_{MNT_s}\|_2 \quad (24)$$

$$\|(v_p)_{MNT_s}\|_2 \leq \gamma_{c_e} \|(\hat{e}_{cl_c})_N\|_2 + \sqrt{\frac{b}{2}} \|(r_c)_N\|_2 \quad (25)$$

in which the final two inequalities were a direct result of (20) and (21) respectively. and substituting (25) into (22) results in

$$E_p \leq \gamma_{c_e} E_c + \left(\frac{1}{\sqrt{2b}} R_p + \sqrt{\frac{b}{2}} R_c \right) \quad (26)$$

similarly substituting (24) into (23) results in

$$E_c \leq \gamma_{p_e} E_p + \left(\frac{1}{\sqrt{2b}} R_p + \sqrt{\frac{b}{2}} R_c \right) \quad (27)$$

Substituting (26) into (27) results in the following

$$E_c \leq \gamma_{p_e} \gamma_{c_e} E_c + (\gamma_{p_e} + 1) \left(\frac{1}{\sqrt{2b}} R_p + \sqrt{\frac{b}{2}} R_c \right)$$

$$E_c \leq \frac{\gamma_{p_e} + 1}{1 - \gamma_{p_e} \gamma_{c_e}} \left(\frac{1}{\sqrt{2b}} R_p + \sqrt{\frac{b}{2}} R_c \right)$$

likewise, substituting (27) into (26) results in the following

$$E_p \leq \gamma_{p_e} \gamma_{c_e} E_p + (\gamma_{c_e} + 1) \left(\frac{1}{\sqrt{2b}} R_p + \sqrt{\frac{b}{2}} R_c \right)$$

$$E_p \leq \frac{\gamma_{c_e} + 1}{1 - \gamma_{p_e} \gamma_{c_e}} \left(\frac{1}{\sqrt{2b}} R_p + \sqrt{\frac{b}{2}} R_c \right)$$

note that the inequalities only result if $\gamma_{p_e} \gamma_{c_e} < 1$. ■

Next we note the following observation that $\gamma_{p_e} = g(\sqrt{2b}H_{p_e}) = g(-\sqrt{2b}H_{p_e})$ and $\gamma_{c_e} = g(\sqrt{\frac{2}{b}}H_{c_e}) = g(-\sqrt{\frac{2}{b}}H_{c_e})$ therefore using Theorem 1, Theorem 2 the following Corollary follows.

Corollary 1:

$$\gamma_{p_e} = g(\sqrt{2b}H_{p_e}) = \max \left\{ \left| \frac{ba_p - 1}{ba_p + 1} \right|, \left| \frac{bb_p - 1}{bb_p + 1} \right| \right\} \quad (28)$$

$$\gamma_{c_e} = g\left(\sqrt{\frac{2}{b}}H_{c_e}\right) = \max \left\{ \left| \frac{b - b_c}{b + b_c} \right|, \left| \frac{b - a_c}{b + a_c} \right| \right\} \quad (29)$$

Therefore:

1. when the plant is passive ($a_p = 0, b_p = \infty$) then $\gamma_{p_e} = 1$ which implies $\gamma_{p_e} \gamma_{c_e} < 1$ if the controller is strictly-input-output-passive $0 < a_c \leq b_c < \infty$ (and vice-versa).
2. when the plant is inside the sector $[a_p, \infty]$ in which $a_p < 0$ then $\gamma_{p_e} \gamma_{c_e} < 1$ if the controller is inside the sector $[a_c, b_c]$ in which $-b^2 a_p < a_c, b_c < \frac{-1}{a_p}$.

As was shown in [10] the *IPESH* blocks can be used to aid with analysis such that

$$\|(e_c)_N\|_2 = \frac{1}{\sqrt{MT_s} K_{MT_s}} \|(e_c)_{MNT_s}\|_2 \quad (30)$$

holds. In addition, the following inequality result from applying the *Schwarz inequality* as demonstrated in [17, proof of Theorem 1-III].

$$\|(r_c)_N\|_2 \leq \sqrt{MT_s} K_{MT_s} \|(r_{ct})_{MNT_s}\|_2 \quad (31)$$

Theorem 3: When $\gamma_{p_e} \gamma_{c_e} < 1$ the digital control network depicted in Fig. 1 is L_m^2 -stable in which there exists a $0 < \gamma < \infty$ such that

$$\|y(t)\|_2 \leq \gamma \|u(t)\|_2$$

in which $y^T(t) = [f_p^T(t), e_{ct}^T(t)]$
and $u^T(t) = [r_p^T(t), r_{ct}^T(t)]$.

Proof: (Sketch) Observe that

$$\|(e_c)_N\|_2 \leq \frac{bb_c}{b + b_c} \sqrt{\frac{2}{b}} E_c$$

holds since H_{cl_c} has finite-gain, therefore

$$\frac{1}{\sqrt{MT_s} K_{MT_s}} \|(e_{ct})_{MNT_s}\|_2 \leq \frac{bb_c}{b + b_c} \sqrt{\frac{2}{b}} E_c$$

holds due to (30). Similarly, observe that

$$\|(f_p)_{MNT_s}\|_2 \leq \frac{b_p}{1 + bb_p} \sqrt{2b} E_p$$

holds since the closed-loop plant H_{cl_p} has finite-gain. Finally, we observe that (31) along with the other continuous-time-norm inequalities can be substituted into the final-two inequalities of Lemma 2 such that both inequalities involve only continuous-time norms in which the outputs $f_p(t)$ and $e_{ct}(t)$ are bounded by the inputs $r_p(t)$ and $r_{ct}(t)$. Therefore, when $\gamma_{p_e} \gamma_{c_e} < 1$ the digital control network depicted in Fig. 1 is L_m^2 -stable. ■

C. Conic Digital Filters

The section shows how an engineer can synthesize a discrete-time controller/filter from a continuous-time reference model. In particular, we show how a continuous-time conic system can be transformed into a discrete-time conic system using the *inner-product equivalent sample and hold (IPESH)*. Additionally, we present a corollary for transforming a continuous-time conic SISO LTI-system into a discrete-time conic SISO LTI-system using the *IPESH-Transform*. We begin by recalling the definition for the *IPESH*.

Definition 2: [18, Definition 4] Let $G_{ct} : L_e^2(U) \rightarrow L_e^2(Y)$ denote an input-output mapping. The *IPESH* may be applied to transform G_{ct} into the discrete-time domain, resulting in the mapping $G_d : l_e^2(U) \rightarrow l_e^2(Y)$, as follows:

- I. $x(t) = \int_0^t y(\tau) d\tau$,
- II. $y(i) = x((i+1)T_s) - x(iT_s)$,
- III. $u(t) = u(i), \forall t \in [iT_s, (i+1)T_s]$.

Remark 1: The inner-product is preserved using the *IPESH* (see [18] for details).

Lemma 3: If H_{ct} is inside the sector $[a, b]$ then H_d resulting from the *IPESH* is inside the sector $[aT_s, bT_s]$.

Proof: Since H_{ct} is inside the sector $[a, b]$, we can write

$$\langle y, u \rangle_T \geq \frac{1}{a+b} \|(y)_T\|_2^2 + \frac{ab}{a+b} \|(u)_T\|_2^2. \quad (32)$$

But, from Definition 2-III it can be shown that

$$\|(u)_T\|_2^2 = T_s \|(u)_N\|_2^2. \quad (33)$$

Additionally, from Definition 2-II and the *Schwarz inequality*, the following inequality can be shown to hold [17, proof of Theorem 1-III]

$$\|(y)_T\|_2^2 \geq \frac{1}{T_s} \|(y)_N\|_2^2. \quad (34)$$

Finally, we use the equivalence of the discrete-time and continuous-time inner products combined with (33) and (34), and substitute into (32) to obtain

$$\begin{aligned} \langle y, u \rangle_N &\geq \frac{1}{T_s(a+b)} \|(y)_N\|_2^2 + \frac{abT_s}{a+b} \|(u)_N\|_2^2 \\ &= \frac{1}{(aT_s) + (bT_s)} \|(y)_N\|_2^2 + \frac{(aT_s)(bT_s)}{(aT_s) + (bT_s)} \|(u)_N\|_2^2, \end{aligned}$$

which proves the result. \blacksquare

At this point we have shown that a continuous-time conic system can be transformed through the *IPESH* into a discrete-time conic system. Since this is a general result, it certainly applies for the special case of conic single-input-single-output (SISO) LTI systems. In this case, the *IPESH-Transform* can be expressed in closed-form as follows.

Definition 3: [4, Definition 5] Let $H_p(s)$ and $H_p(z)$ denote the respective continuous and discrete time transfer functions which describe a plant. Furthermore, let T_s denote the respective sample and hold time. Finally, denote $\mathcal{Z}\{F(s)\}$ as the z -transform of the sampled time series whose Laplace transform is the expression of $F(s)$, given on

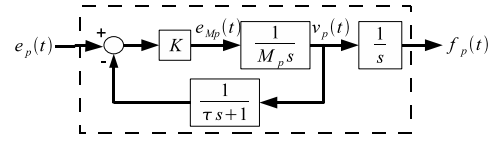


Fig. 5. Plant Dynamics $H_p(s)$

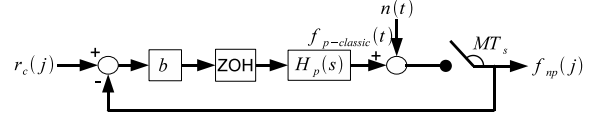


Fig. 6. The classical digital-control-design for position tracking

the same line in [19, Table 8.1 p.600]. $H_p(z)$ is generated using the following *IPESH-Transform*

$$H_p(z) = \frac{(z-1)^2}{T_s z} \mathcal{Z} \left\{ \frac{H_p(s)}{s^2} \right\}.$$

The proof for [4, Lemma 5] shows that the *IPESH-Transform* is a scaled-version ($k = \frac{1}{T_s}$) of the *IPESH* given in Definition 2. Recall the scaling property for conic-systems, which states that if H is inside the sector $[a, b]$, then kH is inside the sector $[ka, kb]$ for any scalar k [5]. Therefore, we have the following corollary:

Corollary 2: If a SISO LTI system $H(s)$ is inside the sector $[a, b]$ then $H_d(z)$ resulting from applying the *IPESH-Transform* is inside the sector $[a, b]$.

III. SINGLE-DEGREE OF FREEDOM TELE-OPERATOR NETWORK

Fig. 5 depicts the idealized *LTI*-model (neglecting gravitational effects) for a single-degree-of-freedom haptic-paddle (with mass M_p) with a proportional (feed-back gain K) filtered-velocity feedback-loop (with filter-time-constant τ) in order for $H_p(s)$ to be inside the sector $[a_p, \infty]$. It can be verified that if

$$K = \frac{M_p}{\tau} \text{ then } H_p(s) \text{ is inside the sector } [-\tau, \infty].$$

This nominal plant-system $H_p(s)$ will be controlled using our digital-control network depicted in Fig. 1 in which we shall use a proportional-controller $e_c(j) = k_c e_r(j)$ in which the gain k_c is chosen to satisfy L_m^2 -stability such that

$$k_c < \frac{1}{\tau} = -\frac{1}{a_p}.$$

In addition K_{MT_s} is chosen so that $r_{ct}(t) = f_p(t)$ at steady-state. We note that $r_p(t)$ is probably better thought of as an over-riding position reference in this frame-work, in which we note that force-disturbances are introduced in the inner-velocity feedback loop and are quickly rejected. In our proposed frame-work, we note that if the robotic-manipulator hits a wall and steady-state error results ($r_c(t) \neq f_p(t)$) the operator receives increased force-feedback $e_c(t)$ which is proportional to this error ($r_c(t) - f_p(t)$). Fig. 6 depicts a classic-digital-position-feedback control scheme in which $r_c(j) = f_{p\text{-classic}}(jMT_s)$ at steady-state if $n(t) = 0$. We chose the feed-back gain to be the same as the

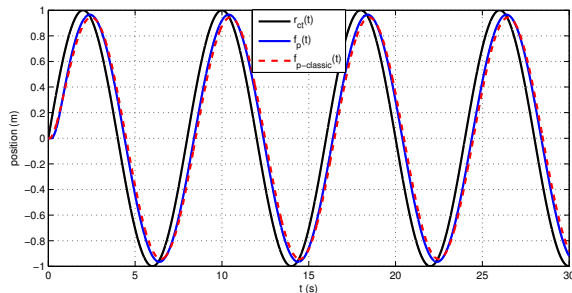


Fig. 7. Baseline tracking response in which $n(t) = 0$.

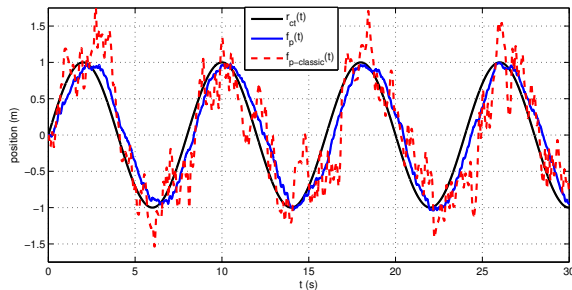


Fig. 8. Position response in which $n(t) \neq 0$.

scattering-gain b in order to get a slightly slower-response than our high-performance system. However, we want to measure how the two systems respond to the introduction of wide-band noise $n(t)$ in which the feed-back signal $f_{np}(j) = f_{p\text{-classic}}(MT_s j) + n(MT_s j)$ for the classical-scheme. For our high-performance system we filter the noise corrupted signal using the multi-rate-passive-sampler subsystem (Fig. 4) described in Section II-B in which $H_{LPC}(s)$ is an analog second-order-low-pass Butterworth-filter in which its center-frequency $\omega_c = \frac{\pi}{MT_s}$ in addition the second-stage digital anti-aliasing filter $H_{LP}(z)$ was synthesized by applying the *IPESH*-Transform to a seventh-order Butterworth-filter model $H_{LP}(s)$ with the same center-frequency ω_c [20, Section 9.7.5].

IV. SIMULATION RESULTS

The simulation parameters are as follows: $b = 2$, $M_p = 2$ kg, $T_s = .01$ seconds, $M = 10$, $\tau = \frac{MT_s}{\pi}$ and $k_c = 30 < 10\pi$. Fig. 7 indicates that our high-performance position $f_p(t)$ response tracks the desired reference $r_c(t)$ closer than the classic-digital-control-system response $f_{p\text{-classic}}(t)$. Fig. 8 indicates the superior advantage our high-performance system has in tracking the desired reference $r_p(t)$ when bandwidth-limited-white-noise is introduced with bandwidth $\frac{10\pi}{T_s}$. Both systems reject steady-state force disturbances as predicted and as previously discussed. In addition, the controller-term $e_{ct}(t)$ in our high-performance-digital control network provides additional force-feedback to an operator if steady-state error occurs while maintaining steady-state operation when the manipulator contacts a wall.

V. CONCLUSIONS

Theorem 1 provides a simple rule to characterize the resulting conic-properties when closing the loop of a conic system inside the sector $[a, b]$. This allowed us to use the reasonable Assumption 1 to analyze the internal-stability structure (Fig. 3) of our proposed high-performance digital control network for continuous time systems depicted in Fig. 2. We showed that a novel-multi-rate *linear*-passive sampler depicted in Fig. 4 satisfied the key-inequality (1) (Lemma 1), combined with a multi-rate-passive-hold system in order to interconnect digital-controllers to continuous time systems and achieve L_m^2 -stability while allowing anti-aliasing filters to be introduced and *not* affect either stability or performance (which traditional anti-aliasing-filters do in classic digital control frameworks). Lemma 2 provides the small-gain conditions, while Corollary 1 demonstrates how non-passive plants inside the sector $[a, \infty]$ can be interconnected to certain strictly-input-output-passive digital controllers in order to attain L_m^2 -stability (Theorem 3). Corollary 2 shows how the *IPESH*-Transform can be applied to a conic-analog-controller inside the cone $[a, b]$ in order to synthesize a conic-digital-controllers inside the sector $[a, b]$. Finally, simulation results of a single-degree-of-freedom haptic paddle using our proposed architecture show good performance even when subject to bandwidth-limited noise.

REFERENCES

- [1] P. Antsaklis and J. Baillieul, Eds., *Special Issue: Technology of Networked Control Systems*, ser. Proceedings of the IEEE. IEEE, 2007, vol. 95 number 1.
- [2] C. A. Desoer and M. Vidyasagar, *Feedback Systems: Input-Output Properties*. Orlando, FL, USA: Academic Press, Inc., 1975.
- [3] N. Kottenstette, X. Koutsoukos, J. Hall, J. Sztipanovits, and P. Antsaklis, "Passivity-Based Design of Wireless Networked Control Systems for Robustness to Time-Varying Delays," *Real-Time Systems Symposium*, 2008, pp. 15–24, 2008.
- [4] N. Kottenstette, J. Hall, X. Koutsoukos, P. Antsaklis, and J. Sztipanovits, "Digital control of multiple discrete passive plants over networks," *International Journal of Systems, Control and Communications (IJSCC)*, no. Special Issue on Progress in Networked Control Systems, 2009, to Appear.
- [5] N. Kottenstette and J. Porter, "Digital passive attitude and altitude control schemes for quadrotor aircraft," Institute for Software Integrated Systems, Vanderbilt University, Nashville, TN, Report, 11/2008 2008, to Appear ICCA09. [Online]. Available: <http://www.isis.vanderbilt.edu/node/4051>
- [6] G. Niemeyer and J.-J. E. Slotine, "Telemanipulation with time delays," *International Journal of Robotics Research*, vol. 23, no. 9, pp. 873 – 890, 2004. [Online]. Available: <http://dx.doi.org/10.1177/0278364904045563>
- [7] R. Anderson and M. Spong, "Asymptotic stability for force reflecting teleoperators with time delay," *The International Journal of Robotics Research*, vol. 11, no. 2, pp. 135–149, 1992.
- [8] G. Zames, "On the input-output stability of time-varying nonlinear feedback systems. i. conditions derived using concepts of loop gain, conicity and positivity," *IEEE Transactions on Automatic Control*, vol. AC-11, no. 2, pp. 228 – 238, 1966.
- [9] J. Willems, *Feedback systems. The analysis of*. London, UK: MIT Press, 1971.
- [10] N. Kottenstette and N. Chopra, "Lm2-stable digital-control networks for multiple continuous passive plants," *1st IFAC Workshop on Estimation and Control of Networked Systems (NecSys'09)*, 09 2009.
- [11] S. Hirche and M. Buss, "Transparent Data Reduction in Networked Telepresence and Teleaction Systems. Part II: Time-Delayed Communication," *Presence: Teleoperators and Virtual Environments*, vol. 16, no. 5, pp. 532–542, 2007.

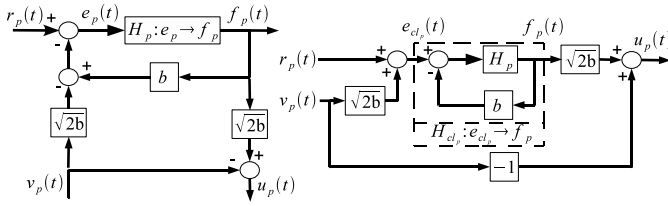


Fig. 9. Plant- r_p - v_p - f_p - u_p -network realization and initial transformation.

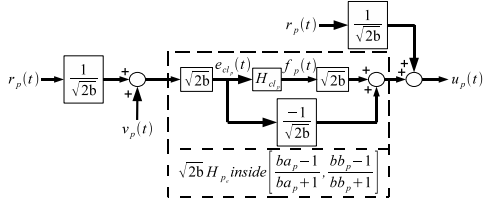


Fig. 10. Final Plant- r_p - v_p - f_p - u_p -network realization.

- [12] N. Chopra, P. Berestesky, and M. Spong, "Bilateral teleoperation over unreliable communication networks," *IEEE Transactions on Control Systems Technology*, vol. 16, no. 2, pp. 304–313, 2008.
- [13] S. Hirche, T. Mafiakis, and M. Buss, "A distributed controller approach for delay-independent stability of networked control systems," *Automatica*, vol. 45, no. 8, pp. 1828–1836, 2009.
- [14] W. M. Haddad and V. S. Chellaboina, *Nonlinear Dynamical Systems and Control: A Lyapunov-Based Approach*. Princeton, New Jersey, USA: Princeton University Press, 2008.
- [15] R. J. Anderson and M. W. Spong, "Bilateral control of teleoperators with time delay," *Proceedings of the IEEE Conference on Decision and Control Including The Symposium on Adaptive Processes*, pp. 167 – 173, 1988. [Online]. Available: <http://dx.doi.org/10.1109/CDC.1988.194290>
- [16] N. Kottenstette, G. Karsai, and J. Sztipanovits, "A passivity-based framework for resilient cyber physical systems," *ISRCS 2009 2nd International Symposium on Resilient Control Systems*, 08 2009.
- [17] N. Kottenstette and P. Antsaklis, "Wireless Control of Passive Systems Subject to Actuator Constraints," *47th IEEE Conference on Decision and Control, 2008. CDC 2008*, pp. 2979–2984, 2008.
- [18] —, "Stable digital control networks for continuous passive plants subject to delays and data dropouts," *2007 46th IEEE Conference on Decision and Control*, pp. 4433–4440, 2007.
- [19] G. F. Franklin, J. D. Powell, and A. Emami-Naeini, *Feedback Control of Dynamic Systems*, 5th ed. Prentice-Hall, 2006.
- [20] A. Oppenheim, A. Willsky, and S. Nawab, *Signals and systems*. Prentice hall Upper Saddle River, NJ, 1997.

APPENDIX

Fig. 9 depicts a graphical realization of (11) on the left-hand-side (LHS), and the first obvious graphical-transformation on the right-hand-side (RHS) in which we denote closed-loop-transformation of the plant H_p in terms of the feedback-gain b as $H_{cl_p} : e_{cl_p} \rightarrow f_p$ in which

$$e_{cl_p}(t) = r_p(t) + \sqrt{2b}v_p(t) = e_p(t) + bf_p(t). \quad (35)$$

In order to simplify discussion and to leverage Theorem 1 we use Assumption 1 in order to state the following corollary:

Corollary 3: If Assumption 1 is satisfied then $H_{cl_p} : e_{cl_p} \rightarrow f_p$ is inside the sector $\left[\frac{a_p}{1+ba_p}, \frac{b_p}{1+bb_p} \right]$. Next we transform the RHS realization in Fig. 9 to the final form depicted in Fig. 10.

Lemma 4: The RHS of Fig. 9 can be transformed to the final form depicted in Fig. 10. In addition if Assumption 1

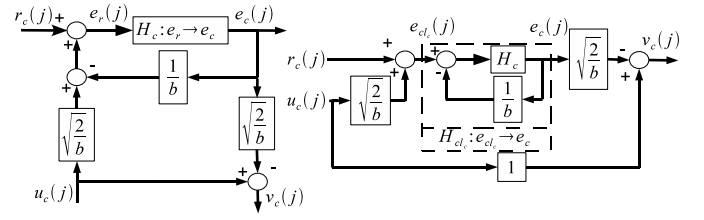


Fig. 11. Controller- r_c - u_c - e_p - v_c -network realization and initial transformation.

is satisfied, then

$$\sqrt{2b}H_{p_e} \text{ is inside the sector } \left[\frac{ba_p - 1}{ba_p + 1}, \frac{bb_p - 1}{bb_p + 1} \right]. \quad (36)$$

Proof: From Fig. 10 it is clear that,

$$e_{cl_p}(t) = \sqrt{2b} \left(\frac{1}{\sqrt{2b}}r_p(t) + v_p(t) \right) = r_p(t) + \sqrt{2b}v_p(t)$$

which satisfies (35), next from Fig. 10 it is clear that,

$$\begin{aligned} u_p(t) &= \sqrt{2b}f_p(t) - \frac{1}{\sqrt{2b}}e_{cl_p}(t) + \frac{1}{\sqrt{2b}}r_p(t) \\ &= \sqrt{2b}f_p(t) - \frac{1}{\sqrt{2b}}(r_p(t) + \sqrt{2b}v_p(t)) + \frac{1}{\sqrt{2b}}r_p(t) \\ &= \sqrt{2b}f_p(t) - v_p(t). \end{aligned}$$

which satisfies (11) in regards to $u_p(t)$. From Corollary 3 we have that $H_{cl_p} : e_{cl_p} \rightarrow f_p$ is inside the sector $\left[\frac{a_p}{1+ba_p}, \frac{b_p}{1+bb_p} \right]$. From the scaling property [5, Property 1-(ii)], we have that sector-properties of $H_{cl_p}\sqrt{2b} = \sqrt{2b}H_{cl_p}$ in which $\sqrt{2b}H_{cl_p}$ is inside the sector $\left[\sqrt{2b}\frac{a_p}{1+ba_p}, \sqrt{2b}\frac{b_p}{1+bb_p} \right]$. Using the sum-rule [5, Property 1-(iii)] we have that

H_{p_e} is inside the sector

$$\left[\frac{-1}{\sqrt{2b}} + \sqrt{2b}\frac{a_p}{1+ba_p}, \frac{-1}{\sqrt{2b}} + \sqrt{2b}\frac{b_p}{1+bb_p} \right]$$

solving for a_{p_e} we have

$$a_{p_e} = \frac{-1}{\sqrt{2b}} + \sqrt{2b}\frac{a_p}{1+ba_p} = \frac{1}{\sqrt{2b}} \left(\frac{2ba_p - ba_p - 1}{ba_p + 1} \right)$$

therefore H_{p_e} is inside the sector

$$\left[\frac{1}{\sqrt{2b}} \left(\frac{ba_p - 1}{ba_p + 1} \right), \frac{1}{\sqrt{2b}} \left(\frac{bb_p - 1}{bb_p + 1} \right) \right]$$

finally from the scaling property we have that

$$\sqrt{2b}H_{p_e} \text{ is inside the sector } \left[\frac{ba_p - 1}{ba_p + 1}, \frac{bb_p - 1}{bb_p + 1} \right].$$

Fig. 11 depicts a graphical realization of (12) on the left-hand-side (LHS), and the first obvious graphical-transformation on the right-hand-side (RHS) in which we denote closed-loop-transformation of the controller H_c in terms of the feedback-gain $\frac{1}{b}$ as $H_{cl_c} : e_{cl_c} \rightarrow e_c$ in which

$$e_{cl_c}(j) = r_c(j) + \sqrt{\frac{2}{b}}u_c(j) = e_r(j) + \frac{1}{b}e_c(j). \quad (37)$$

Which allows us to state the following corollary:

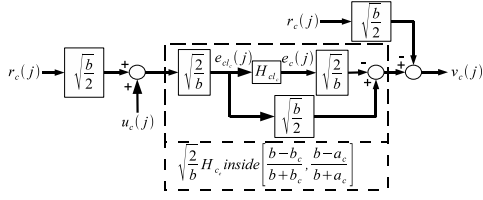


Fig. 12. Final Controller- r_c - u_c - e_c - v_c -network realization.

Corollary 4: If Assumption 1 is satisfied then $H_{cl_c} : e_{cl_c} \rightarrow e_c$ is inside the sector $\left[\frac{ba_c}{b+a_c}, \frac{bb_c}{b+b_c} \right]$. Next we transform the RHS realization in Fig. 11 to the final form depicted in Fig. 12.

Lemma 5: The RHS of Fig. 11 can be transformed to the final form depicted in Fig. 12. In addition if Assumption 1 is satisfied, then

$$\sqrt{\frac{2}{b}} H_{c_e} \text{ is inside the sector } \left[\frac{b-b_c}{b+b_c}, \frac{b-a_c}{b+a_c} \right].$$

Proof: From Fig. 12 it is clear that,

$$e_{cl_c}(j) = \sqrt{\frac{2}{b}} \left(\sqrt{\frac{b}{2}} r_c(j) + u_c(j) \right) = r_c(j) + \sqrt{\frac{2}{b}} u_c(j)$$

which satisfies (37), next from Fig. 12 it is clear that,

$$\begin{aligned} v_c(j) &= -\sqrt{\frac{2}{b}} e_c(j) + \sqrt{\frac{b}{2}} e_{cl_c}(j) - \sqrt{\frac{b}{2}} r_c(j) \\ &= -\sqrt{\frac{2}{b}} e_c(j) + \sqrt{\frac{b}{2}} \left(r_c(j) + \sqrt{\frac{2}{b}} u_c(j) \right) - \sqrt{\frac{b}{2}} r_c(j) \\ &= -\sqrt{\frac{2}{b}} e_c(j) + u_c(j). \end{aligned}$$

which satisfies (12) in regards to $v_c(j)$. From Corollary 4 we have that $H_{cl_c} : e_{cl_c} \rightarrow e_c$ is inside the sector $\left[\frac{ba_c}{b+a_c}, \frac{bb_c}{b+b_c} \right]$. From the scaling property, we have that sector-properties of $-H_{cl_c} \sqrt{\frac{2}{b}} = -\sqrt{\frac{2}{b}} H_{cl_c}$ in which $-\sqrt{\frac{2}{b}} H_{cl_c}$ is inside the sector $\left[-\sqrt{\frac{2}{b}} \frac{bb_c}{b+b_c}, -\sqrt{\frac{2}{b}} \frac{ba_c}{b+a_c} \right]$. Using the sum-rule we have that

H_{c_e} is inside the sector

$$\left[\sqrt{\frac{b}{2}} - \sqrt{\frac{2}{b}} \frac{bb_c}{b+b_c}, \sqrt{\frac{b}{2}} - \sqrt{\frac{2}{b}} \frac{ba_c}{b+a_c} \right]$$

solving for b_{c_e} we have

$$b_{c_e} = \sqrt{\frac{b}{2}} - \sqrt{\frac{2}{b}} \frac{ba_c}{b+a_c} = \sqrt{\frac{b}{2}} \left(1 - \frac{2a_c}{b+a_c} \right)$$

therefore H_{c_e} is inside the sector

$$\left[\sqrt{\frac{b}{2}} \left(\frac{b-b_c}{b+b_c} \right), \sqrt{\frac{b}{2}} \left(\frac{b-a_c}{b+a_c} \right) \right]$$

finally from the scaling property we have that

$$\sqrt{\frac{2}{b}} H_{p_e} \text{ is inside the sector } \left[\frac{b-b_c}{b+b_c}, \frac{b-a_c}{b+a_c} \right].$$

■